Assessment of performance of dynamic compaction with numerical simulations

Houman Soleimani Fard
Keller Grundbau GmbH, Dubai, UAE

GeoCalgary 2022 October 2-5
Reflection on Resources

ABSTRACT
Thanks to its simplicity and affordability, dynamic compaction (DC) is one of the most widely used ground improvement techniques. Compactability of soils subjected to DC is a function of fines content, moisture content, initial void ratio, compaction parameters, etc. The best way to evaluate DC performance is to carry out a trial campaign in which various compaction schemes are applied and assessed by penetration tests (usually CPT) prior to and after the compaction. Yet, there is no unanimously accepted method to convert the pre-improvement to the post-improvement ground condition taking the compaction scheme into account. In this paper the DC technique is briefly introduced, and an attempt is made to numerically analyze the changes in the soil conditions during a DC work using PLAXIS software. The CPT tests executed in both untreated and compacted grounds are modelled to calculate the achieved improvement. The numerical outcomes are compared with the test results and demonstrated good matches with the actual soil improvement performance observed in a real DC project.

RÉSUMÉ
La méthode de compactage dynamique (DC), grâce à sa simplicité et son coût raisonnable, est l'une des techniques d'amélioration des sols les plus utilisées. La compressibilité des sols soumis au DC est fonction de la quantité de particules fines, de la teneur en eau, du niveau de vide initial, des paramètres de compactage, etc. La meilleure façon d'évaluer la performance de la DC est d'effectuer une campagne d'essais dans laquelle différents schémas de compactage sont appliqués et évalués par des tests de pénétration (généralement CPT) avant et après le compactage. Pourtant, on ne dispose pas d'une méthode universellement acceptée pour convertir l'état du sol avant l'amélioration en état après l'amélioration en tenant compte du schéma du tassement. Dans cet article, la technique DC est présentée brièvement et on essaie d'analyser numériquement les changements dans les conditions du sol durant une intervention DC en utilisant le logiciel PLAXIS. Les tests CPT exécutés dans les sols non traités et compactés sont modélisés pour calculer l'amélioration obtenue. Les résultats numériques sont comparés avec les essais et montrent une bonne corrélation avec le résultat obtenu par l'amélioration du sol observée dans un véritable projet de DC.

1 INTRODUCTION

Dynamic Compaction (DC) is a ground improvement technique that densifies soils by releasing a 10-30-ton pounder (rarely heavier) multiple times from a height of 5-30 m. The ground is subjected to repeated surface tamping in a uniform grid of compaction points called “prints” or “craters” (Figure 1). Depending on soil type, improvement depth and project specification prints are usually 3-7 m spaced (less commonly denser or wider). After the compaction procedure is completed, the open craters and the surface should be backfilled (if needed) and graded. Next, the final phase of compaction, named ironing, should be conducted in which a flat pounder is released from a relatively shorter height to compact the area between the prints and homogenize the ground. Ironing usually scans the whole surface. As a result of dynamic compaction void ratio of the soil reduces to different levels depending on the depth, size and shape of crater and initial condition of the soil. This densification enhances the modulus of elasticity and internal friction angle.

No imported material is needed in typical DC, therefore, it is considered as an environmentally friendly solution and recommended wherever applicable. Conversely, this technique is time-consuming or inapplicable for soils containing more than 25-30% fine content. Another limitation of this technique is the influence depth, which hardly goes beyond 8-12 m (depending on soil condition and compaction scheme). Nonetheless, DC is widely implemented for the uniform and general treatment of loose sands to silty sands and newly backfilled grounds (e.g., Kirsch and Bell 2019). The load-bearing capacity of DC-treated grounds is typically less than that of other ground improvement techniques like vibro stone columns or deep soil mixing.

Cone Penetration Test (CPT) is the most widely employed test to evaluate the post-DC condition of compacted soils. As quality requirements of DC-treated grounds; either a target curve is defined for the CPT cone resistance (q_c), or functional requirements (e.g., bearing capacity, static settlement, liquefaction, etc.) have to be complying with project specification. In the latter case among all depth investigations, CPT -in spite of having some limitations- provides the most accurate data for further correlations and calculations (e.g., Robertson 2009 and 2016, and particularly for DC Shen et al. 2018 and Shen et al. 2019).

Figure 1. DC craters and a pounder

During compaction and due to the imposed deformation, excess pore water pressure is built up in the soil. Regarding the soil type (usually silty sand with lenses of fine-grained soils) dissipation of the mobilized excess water pressure may take few days. Therefore, it is strongly recommended to allow at least 4-8 days resting time after compaction and before starting with quality control CPTs.

A comprehensive trial campaign -with various compaction schemes (i.e., number of blows, prints spacing, weight and height of drops)- is recommended to assess the most favorable compaction scheme with respect to the soil condition and project needs. The drops can be split into several passes (drops on the same print but after some resting times) and phases (drops on new prints in between the existing prints).

Figure 2 illustrates first, second and third phases of trial works in a DC project. The proposed CPT locations on the prints and also in between are shown in this figure.

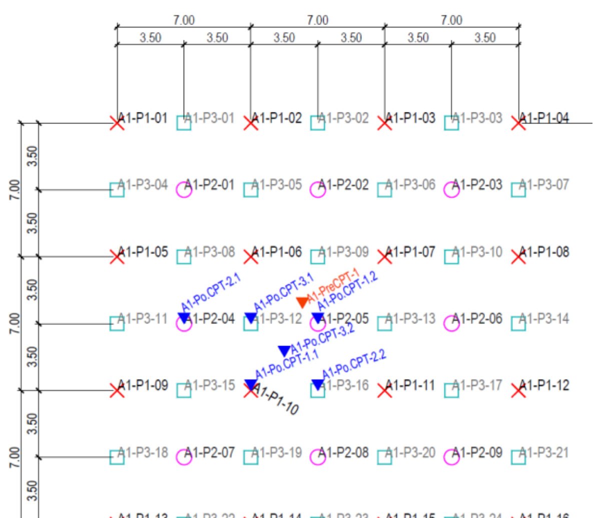

Figure 2. Typical pattern for DC phases and proposed CPT locations. Primary, secondary and tertiary phases are shown by crosses, circles and squares, respectively

In this paper in order to predict post-DC CPT results (or simply post-CPT), two single-print compactions have been numerically simulated. CPT tests were also modelled before and after DC works. The modelling inputs were pre-DC CPT (or simply pre-CPT) as well as depth and width of the prints. The calculated CPT results showed relatively good matches with the field CPT data for the selected conditions. This will allow engineers to model a multi-print compaction and estimate the post-CPTs from prints dimension and pre-CPTs.

2 NUMERICAL STUDIES

2.1 Modelling CPT

Several researchers attempted to model CPT penetration numerically (e.g., Ahmadi 2000, Jarast and Ghayoomi 2018, Kiousis et al. 1988, and Schweiger et al. 2018 among others). The most significant challenges that such simulations are encountered with are the complexity of the model and the large deformations (mesh distortion) as well as the solution schemes (e.g., stress and deformation history in the soil, appropriate material models, tension in soil, soil-rod interfaces, etc.).

Modelling a continuous penetration for the cone into the soil with a constant rate of -usually- 20 mm/s is a realistic approach of simulation of CPT. However, regarding the complexity of model, in this research a simplified method of modelling CPT was employed, in which the cone does not penetrate throughout the depth in one run, but only 20 mm at consecutive and independent steps. First, the CPT cone and rod was modelled at a given depth. In the next phase of modelling, to simulate the penetration, a vertical displacement of 20 mm over one second was imposed on top of the rod. The mobilized vertical stress at top of the rod was considered as an indicator for the q_c (not q_c itself). Then the CPT rod and cone was extended (re-modelled) to the next measurement level, the mesh was updated, and another 20 mm displacement was imposed. The same procedure was repeated to cover the whole investigation depth. The friction between CPT and soil was ignored and the soil-rod interface could transfer only normal stress between the two bodies. The modelling was carried out using PLAXIS 2D v.21.

This modelling approach fails to capture some aspects of the CPT test. In order to minimize the effect of the modelling limitations, the calculated vertical stress in the rod (here named q_c) should not be considered directly as q_c, but can be compared with a reference σ_c calculated in the same way. In this study, σ_c before and after DC (here named $\sigma_{c,pre}$ and $\sigma_{c,post}$, respectively) are calculated and compared. The improvement ratio ($R_i = \sigma_{c,post}/\sigma_{c,pre}$) is logically less sensitive to the modelling shortcomings, hence we assumed here:

$$R_i = \sigma_{c,post}/\sigma_{c,pre} \approx q_{c,post}/q_{c,pre} \quad (1)$$

2.2 Studied Conditions

Two single-print DC cases were studied with the subsoil profiles as explained below. The assigned soil parameters are listed in Table 1 and Table 2. Hardening Soil behavior model (HS) was used for modelling the soils. CPTs conducted on unimproved grounds are plotted in Figure 6 (pre-CPT).

In the first case study the top 8 m of the ground consisted of relatively homogeneous silty Sand with q_c ranging around 4 to 10 MPa increasing by depth, followed by a soft silty layer which was below the influence depth of DC. The fines content of the silty Sand layer was limited to 20%, hence this material should be compactable by DC technique.

Unlike the case 1, the ground of the second case study was composed of compactable and non-compactable strata both within the DC influence depth. The subsoil profile consisted of 2.6 m silty Sand on the top followed by ~0.7 m soft Silt, ~1.5 m silty Sand and again soft Silt starting from depth of 5.7 m. DC should be efficient for the upper silty Sand layer, however, the compactable material underneath the soft Silt may not receive enough compaction energy from the surface as the soft layer act as a damper and absorbs most of the DC energy and vibration.

Table 1. Case study 1: soil profile and properties

Layer	Depth [m]	E [MPa]	m [-]	c' [kPa]	φ' [°]	k [m/s]
Silty Sand	0.0 – 8.0	12	0.50	5	35	1e-6
Silt	> 8.0	1.5	0.55	25	25	2e-8

Table 2. Case study 2: Soil profile and properties

Layer	Depth [m]	E [MPa]	m [-]	c' [kPa]	φ' [°]	k [m/s]
Silty Sand	0.0 – 2.6	12	0.50	5	35	1e-6
Silt	2.6 – 3.3	1.5	0.55	25	25	2e-8
Silty Sand	3.3 – 5.7	12	0.50	5	35	1e-6
Silt	> 5.7	1.5	0.55	25	25	2e-8

Where E represents E_{50}^{ref} and E_{oed}^{ref} of HS model, E_{ur}^{ref} is assumed to be $3 \times E_{50}^{ref}$, m is the exponent of HS model, c' and φ' are shear strength parameters, k denotes permeability and p^{ref} (reference pressure) is 100 kPa for all layers. c', φ' and k values were estimated from the CPT and BH results as given in the geotechnical investigation report of the project.

Moduli of elasticity were correlated using Bowles estimation as follows: $E = \alpha q_c$ where α was assumed to be 3 in this study.

The compaction scheme (i.e., number and height of drops and weight of pounder) was not part of the study, instead the resulting diameter and depth of the craters were considered for calculations. The modelled crater (for both cases) was a 1.2 m deep and 2 m wide. Typically, craters are deeper, but for this study only the first pass of blows were applied.

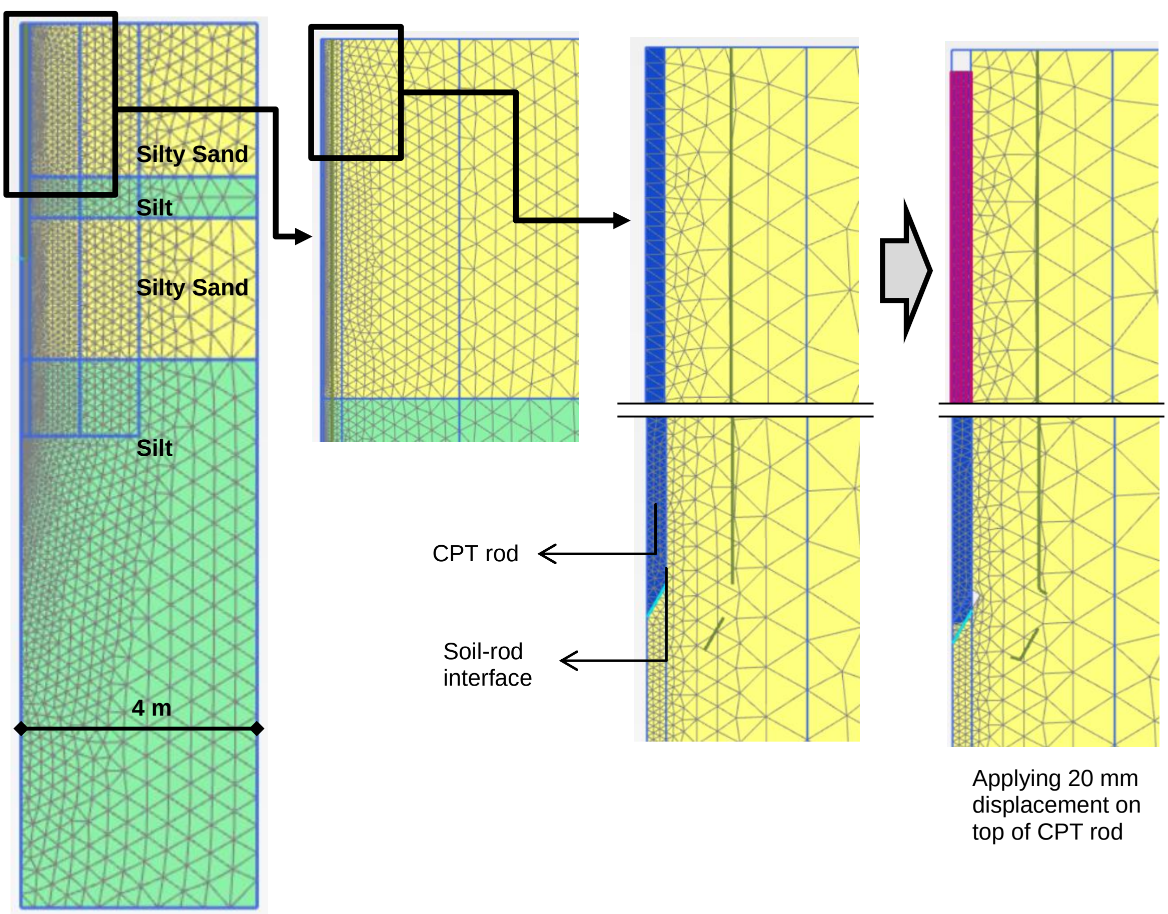

Figure 3. Geometry of the model (case 2)

The compaction process was modelled by imposing this predefined displacement on top of the ground (to model the print crater) followed by a resting period of 5 days for dissipation of the generated excess pore water pressure before modelling the CPT tests. The compaction and testing sequences were as per the actual procedure adopted on site. Taking the soil behavior model used in this study (i.e., HS) into account, at the post-DC condition some residual deformations have been developed within the influence depth of DC, void ratio has reduced, and consequently the modulus of elasticity of compacted soil has improved.

In this study CPT tests, with the abovementioned modelling concept, were simulated in both pre- and post-DC conditions. The CPT cone was 35.7 mm in diameter and 60° in tip angle (one of most commonly used cone types) which was penetrating into the ground with a constant speed of 20 mm/s. The material assigned to the CPT rod was linear elastic with modulus of elasticity of 200 GPa (modulus of elasticity of steel). Depths of CPT penetration were selected so as to cover the influence depth of DC. Axisymmetric models with 4 m width were developed to simulate the geometries as illustrated in Figure 3.

3 RESULTS AND DISCUSSIONS

The deformation imposed during DC changes the stress condition of ground. The minimum principal stress (σ'_3) increases due to the energy applied on the surface; and consequently, regarding the Hardening Soil principles (Eq. 2), the deformation moduli of ground improve. The calculated post-DC σ'_3 is shown in Figure 4 for cases 1 and 2.

$$E_{50} = E_{50}^{ref}\left(\frac{c \cdot \cos\varphi - \sigma'_3 \cdot \sin\varphi}{c \cdot \cos\varphi + p^{ref} \cdot \sin\varphi}\right)^m \tag{2}$$

From another point of view, the applied DC energy preloads the ground and increases the over consolidation ratio (OCR). Hence, in the following cycles of loading (e.g., the operational load) considerably less settlement is expected. All these improvements can be captured numerically by increase in CPT tip resistance as modelled in this study.

In this study the calculated mobilized stress in the rod, denoted by σ_c (or calculated q_c) does not directly represent the field q_c values. The dissimilarities between σ_c and q_c are rooted in the modelling shortcomings and limitations. For example the lateral displacement of the soil due to downward penetration of the cone (which increases the stiffness in hardening soils) is missing. Another imperfection is not taking the stress history of the previous penetration steps into consideration. Moreover, the localized fractures occurring in the soil around an advancing CPT cone cannot be fully modelled in the FEM analysis. In order to minimize the impact of modelling limitations, the calculated σ_c values of the compacted soil were compared with that of the natural (uncompacted) condition.

Pre- and post-DC CPT results of the case studies are plotted in Figure 5. In case 1 the subsoil profile comprises a uniform sandy soil for top 8 m underlain with a soft silty layer. The DC influence depth for case 1 was around 7 to 8 m, as a function of depth. Case 2, however, contained multiple layers of sandy and silty soils as shown in Figure 5. The improvement below the upper silty soil was negligible as plastic materials (e.g., fine grained soils) can damp the applied DC energy instead of transferring that to the lower layers.

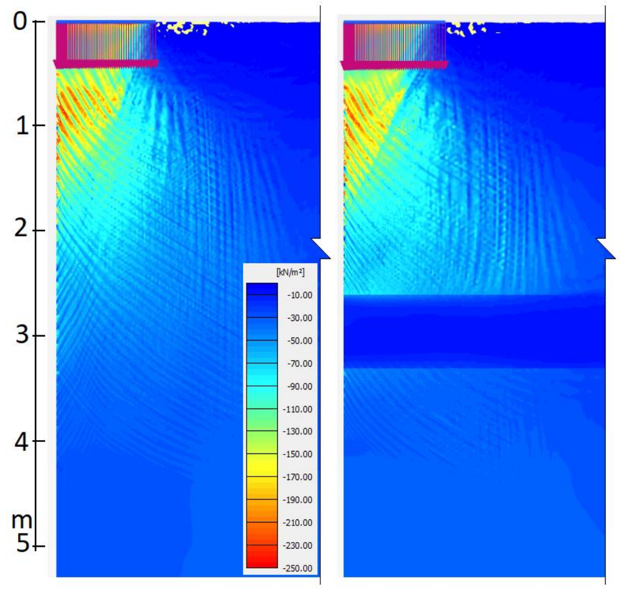

Figure 4. Minimum effective principal stress (σ'_3) in post-DC condition

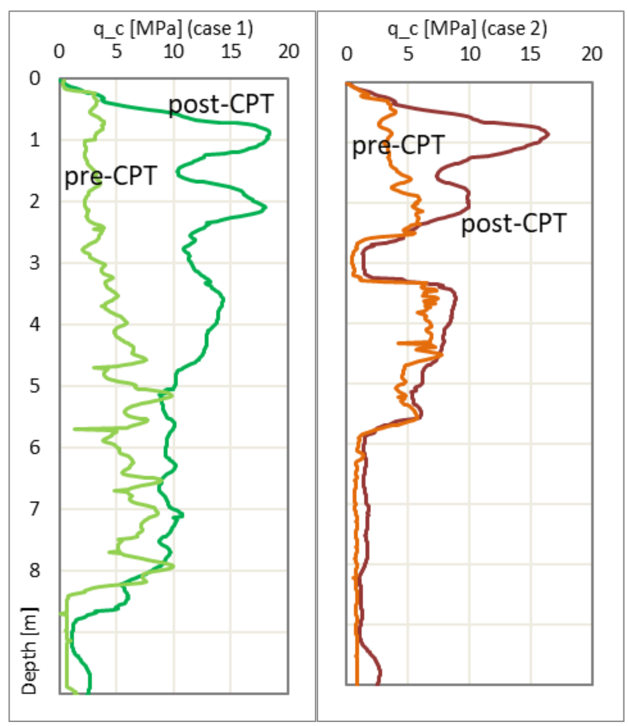

Figure 5. Measured pre- and post-CPT results (q_c)

In Figure 6 the calculated stresses in the CPT rod at the penetration phases (σ_c) of both cases are illustrated. As mentioned earlier σ_c and q_c are not equal, however, their behaviors (e.g., improvement ratio due to DC, $R_i = q_{c,post}/q_{c,pre}$) are expected to follow the same trend. In the studied cases R_i was in the range of 4 to 1 over depths of 0 to 7 m for case 1, and 0 to 2.6 m for case 2. The FEM studies resulted in slightly higher R_i values: 4.4 to 1 for both cases. Moreover, in case 2 some improvement with R_i of 1.6 to 1.2 for the sandy layer below the silty material (depth of 3.3 to 5.7 m) has occurred which was not observed in the field data.

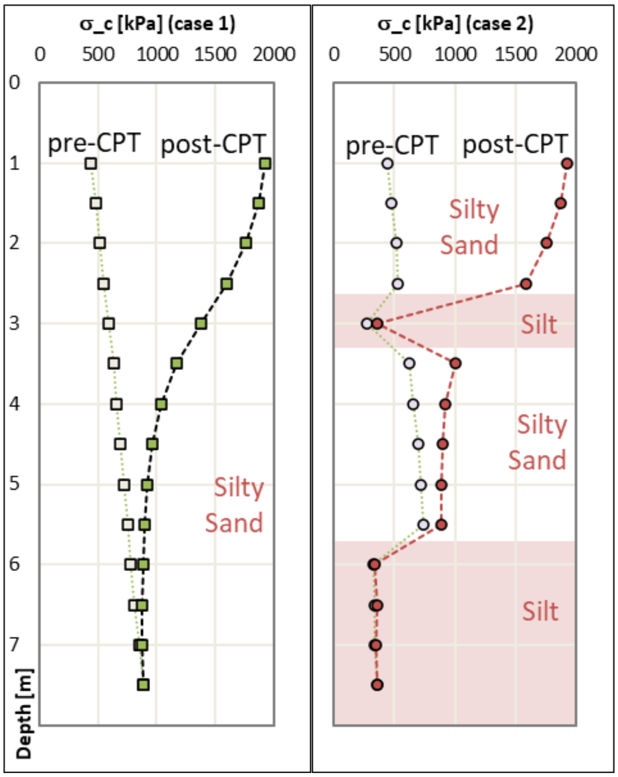

Figure 6. Calculated pre- and post-CPT results (σ_c)

In case 2 the calculations show only 30% growth in σ_c inside the silty soil, whereas, in case 1 this value was around 85% in the sandy layer at the same depth (i.e., 3.5 m). This could be due to the lower permeability of silt compared to that of sand. The craters are assumed to be formed in 5 minutes which is not enough time for the excess pore water pressure to get dissipated. Therefore, no volumetric strain is likely to take place in the silt and the imposed deformation on the surface (i.e., the DC crater) manly displaces the low permeability materials horizontally and vertically rather than densify them. This deformation also damps the compaction energy, instead of transferring to the underlaying compactable layers.

In simulation of both studied cases, the same material was considered for the depths of 3.3 to 5.7 (silty Sand as presented in Table 1 and Table 2), however, the post-CPT σ_c values were up to 17% higher in case 1 where -unlike case 2- there was no shallow silty soil. This can be considered as damping effect of the plastic layers. Although, for the same thickness the difference between the q_c values of the two cases were more visible. As shown in Figure 5, over the depth 3.3 to 5.7 m the increase in the CPT q_c after compaction has been considerably higher for case 1 compared to that in case 2.

4 CONCLUSIONS AND RECOMMENDATIONS

In this paper, an attempt was made to numerically simulate two single-print DC cases based on pre-CPT ground conditions using PLAXIS 2D. Although the calculated vertical stresses in the CPT rod (σ_c) before and after DC were not in the same range as q_c of the actual CPTs, but the improvement ratio and the trend of the results over the depth was reasonably similar in the field results and in the numerical outcomes.

The studied methodology will allow engineers to estimate the post-DC quality of the ground based on the pre-CPTs and the size of the craters. Moreover, such calculations enable engineers to target crater shapes to achieve a minimum required q_c based on the available pre-CPT results.

For a uniformly treated ground with large number of craters, 3D analysis with the same approach as described in this paper can be conducted. In the modeling of a uniform treatment, sequence of work (e.g., order of compaction phases, resting periods, etc.) are of great importance and can influence the numerical results.

More detailed analysis is needed to increase the accuracy of the method; for instance, soil type as identified by soil behavior index (I_c), Atterberg limits, grading, etc. can also be taken into consideration.

Dynamic analysis of the blows based on actual damping and energy dissipation behavior of the ground can further develop the assessment of DC performance.

REFERENCES

Ahmadi, M.M. 2000. *Analysis of cone tip resistance in sand*, Ph.D. thesis, University of British Columbia, Vancouver, Canada.

Jarast, P. and Ghayoomi, M. 2018. Numerical Modeling of Cone Penetration Test in Unsaturated Sand inside a Calibration Chamber, *International Journal of Geomechanics*, ASCE, 18, no. 2, 04017148-1-13, doi: 10.1061/(ASCE)gm.1943-5622.0001052.

Kiousis, P.D., Voyiadjis, G.Z. and Tumay, M.T. 1988. A large strain theory and its application in the analysis of the cone penetration mechanism, *International Journal of Numerical Analysis Methods Geomechanics*, 12, no. 1, 45–60, doi: 10.1002/nag.1610120104.

Kirsch, K. and Bell, F. 2019. *Ground Improvement*, CRC Press. ISBN 9780367865696

Robertson, P.K. 2009. CPT interpretation – a unified approach. *Canadian Geotechnical Journal*, 46, no. 11, 1337–1355, doi: 10.1139/T09-065

Robertson, P.K. 2016. Cone penetration test (CPT)-based soil behaviour type (SBT) classification system – an update. *Canadian Geotechnical Journal*, 53, no. 12. 1–18, doi: 10.1139/cgj-2016-0044

Schweiger, H.F., Fabris, C., Ausweger G., and Hauser, L. 2018. Examples of successful numerical modelling of complex geotechnical problems, *Innovative Infrastructure Solutions*, 4, no. 1, doi: 10.1007/s41062-018-0189-5

Shen, M., Juang, C.H., and Chen, Q. 2019. Mitigation of liquefaction hazard by dynamic compaction - a random field perspective, *Canadian Geotechnical Journal*. 56, no. 12, 1803-1815, https://doi.org/10.1139/cgj-2018-0502

Shen, M., Martin, J.R., Ku, C.-S and Lu, Y.-C. 2018. A case study of the effect of dynamic compaction on liquefaction of reclaimed ground, *Engineering Geology*, 240, 48-61, doi:10.1016/j.enggeo.2018.04.003

Soleimani Fard, H. and Chang, N. 2022. CPT in Layered Soils and Correction of Thin-Layer Effect, *Proc. of 7th International Conference on Geotechnical Research and Engineering*, doi: 10.11159/icgre22.204